Spatial and temporal patterns at small scale in Austrocedrus chilensis *diseased forests and their effect on disease progression*

Ludmila La Manna & Silvia Diana Matteucci

European Journal of Forest Research

ISSN 1612-4669

Eur J Forest Res
DOI 10.1007/s10342-012-0617-6

Springer

Eur J Forest Res
DOI 10.1007/s10342-012-0617-6

ORIGINAL PAPER

Spatial and temporal patterns at small scale in *Austrocedrus chilensis* diseased forests and their effect on disease progression

Ludmila La Manna · Silvia Diana Matteucci

Received: 1 September 2011 / Revised: 12 January 2012 / Accepted: 17 February 2012

Abstract *Austrocedrus chilensis* is an endemic conifer of Patagonia that suffers a widespread mortality whose causes are a topic of discussion. Since *Phytophthora austrocedrae* is the most probable cause, we proposed that the spatial and temporal patterns of disease at small scale should reflect pathogen behavior. We aimed at characterizing the spatial and temporal patterns of diseased trees in different soil types and the effect of microsite variability on diseased trees spatial pattern. The spatial pattern of disease was influenced by soil type and tree density. In clay soils with low disease incidence (ca. 25%), the spatial pattern was random and not influenced by abiotic microsite conditions. When disease incidence increased (ca. 70%), concurring with denser plots, the spatial pattern was clustered, as a result of an infection process, and it was independent of microsite variability. In soils with better drainage conditions, that is, alluvial soils with volcanic ash input and coarse textured volcanic soils, the disease was clustered and associated with flat microtopographies. The progression of the disease at small scale was influenced by soil, precipitation and tree density. The spatial and temporal patterns of disease progression were associated with a contagion process and with environmental variables that affect drainage, coinciding with *Phytophthora* biology and requirements. Our results concur in pointing at *Phytophthora* as the cause of *A. chilensis* disease in the study area. Management practices should be urgently applied in order to minimize the spread of the inoculum.

Keywords Soil · O-ring · Abiotic factors · *Phytophthora*

Communicated by R. Matyssek.

L. La Manna (✉)
Centro de Investigación y Extensión Forestal Andino Patagónico (CIEFAP) and Universidad Nacional de la Patagonia San Juan Bosco (UNPSJB), Ruta 259 Km 4, C.C. 14, 9200 Esquel, Chubut, Argentina
e-mail: llamanna@ciefap.org.ar

L. La Manna
Consejo Nacional de Investigaciones Científicas y Técnicas (CONICET), Esquel, Chubut, Argentina

S. D. Matteucci
CONICET, Grupo de Ecología del Paisaje y Medio Ambiente, Universidad de Buenos Aires, Ciudad Universitaria, Pabellón 3, Piso 4, 1428 Buenos Aires, Argentina
e-mail: sdmatteucci@conicet.gov.ar

Introduction

Austrocedrus chilensis [(D. Don) Pic. Serm.and Bizzarri] is an endemic conifer of the Andean forests of southern Argentina and Chile. In Argentina, it is distributed between 37°7′ and 43°44′S and covers ca. 141,000 ha spreading over a steep west–east precipitation gradient (Pastorino et al. 2006) and on different soil types (La Manna 2005).

This forest species suffers a widespread mortality locally known as "mal del ciprés". Tree symptoms are withering and defoliation, crown thinning and finally, the death of the tree. Two patterns of disease development were recorded: (1) necrotic lesions in the inner bark of roots and root collar, extending up the bole, which is the most frequent, and (2) symptoms first present in the crown as dieback, with only healthy tissues at the root collar (Greslebin and Hansen 2010). The first type of disease pattern was proved to be caused by *Phytophthora austrocedrae* Gresl. and E. M. Hansen (Greslebin and Hansen 2009, 2010). However, El Mujtar (2009) proposed that *P. austrocedrae* acts as a secondary agent and that cavitation is the cause of the disease. Other hypothesis about the

Published online: 04 March 2012

origin of the disease, as forest decline (Calí 1996; Filip and Rosso 1999; La Manna and Rajchenberg 2004a, b) and climatic causes (Calí 1996; Mundo et al. 2010) were also suggested.

The importance of abiotic factors in relation to the disease was shown. The disease is clearly associated with site features, particularly with poor drainage conditions at both microsite (Baccalá et al. 1998; La Manna and Rajchenberg 2004 a, b) and landscape scales (La Manna et al. 2008, 2012). This association with poor drainage may be related to *P. austrocedrae*, since it is an aquatic mold that requires water for dispersion (Greslebin et al. 2007).

The spatial pattern of *A. chilensis* disease at landscape scale is characterized by discrete patches with adjacent asymptomatic trees (La Manna et al. 2012). In two stands located in Nahuel Huapi National Park, tree death occurred in clusters when incidence was lower than 63%, and random when the incidence was higher (Rosso et al. 1994). Field observations suggest that the degree of aggregation varies according to the soil type (La Manna and Rajchenberg 2002). Although results of studies about spatial pattern, dispersion and dynamics of disease process were key for understanding forest disease in other parts of the world (Acker et al. 1996; Hennon et al. 1990; Manion 1991; Shurtleff and Averre 1997), our knowledge about these aspects in *A. chilensis* forests is scarce and results have a great variability (Amoroso and Larson 2010). In biology, the observed patterns and their changes are important indicators of the underlying processes (Tilman 1988; Turner 1989; Wiegand et al. 2003).

Abiotic factors varying at microsite scale are strongly related to *A. chilensis* disease (La Manna and Rajchenberg 2004a, b); however, their influence on the disease spatial and temporal patterns is yet unknown.

In this study, we aimed at characterizing the spatial and temporal patterns of diseased trees in different soil types, and the effect of microsite variability on diseased trees spatial pattern. We proposed that if *P. austrocedrae* is the cause of the disease, the spatial and temporal patterns of disease should reflect pathogen requirements. We hypothesized that the spatial pattern of *A. chilensis* disease at stand level is associated with edaphic features that affect the drainage. We predict a random pattern in clay soils, and in clusters, associated with poor drained microsites, in allophanic soils with courser textures. We also hypothesized that the spatial and temporal patterns of disease progression are associated with a contagion process and with environmental variables that affect the drainage. We predict that trees that become diseased in a short time period (3 years) are those closest to diseased trees, and that the rate of disease progression increases in wetter years.

Materials and methods

Study area

The study was carried out in Río Grande Valley (Futaleufú River), Chubut province, Argentina, located at 43°12′S latitude. Three sampling sites with pure *A. chilensis* forests affected by *P. austrocedrae* were selected according to the differences in morphogenesis and soil type (La Manna and Rajchenberg 2004b; La Manna 2005) (Fig. 1). Site A is located in a large area of glacifluvial deposits, Site B is located next to Río Grande river shore, and Site C corresponds to a glacial eroded landscape, with volcanic and rocky soils. The alphabetic order of sites identification corresponds to a gradient of textures and drainage conditions (La Manna 2005).

The study area presents a steep west–east precipitation gradient. Precipitations are concentrated in autumn and winter (April through August) and diminish markedly toward the summer (i.e., Mediterranean climate). Study sites are located in areas with 1,100- to 1,300-mm mean annual precipitation. According to weather stations of the area, 2007 was a dry year, with rainfalls 60–75% lower than the historical average. On the contrary, in 2008 and 2009, rainfall was 15–35% higher than the historical average. Figure 2 shows the distribution of precipitations during the study period registered by the Futaleufú dam weather station.

Plot description

In each site, two 40 × 60 m plots with disease symptoms were established. All the plots corresponded to dense forests closed to cattle, with no history of logging and where cutting was prevented during the study. The topography and the soil of each plot were described in detail. The distance and slope between systematically distributed points were measured in order to build a digital terrain model of the plot. The model was built using the Spatial Analyst tool of the software ArcView. A pit was dug outside of the plot, and the soil profile was described according to USDA (Schoeneberger et al. 1998). Each plot was divided into 10 × 10 m subplots for microsite characterization. In each subplot, the soil profile was described extracting a complete profile section with an auger. The texture and the reaction to sodium fluoride (NaF) of each horizon were determined in the field according to the methods described by Brady (1974) and Fieldes and Perrot (1966), respectively. The reaction to NaF allows detecting amorphous constituents (i.e., allophane, imogolite) of volcanic ash. Composite soil samples were obtained at 0–20 cm, 60–80 cm and 100–120 cm depth, in four subplots (20 × 20 m). Soil samples were air-dried, and

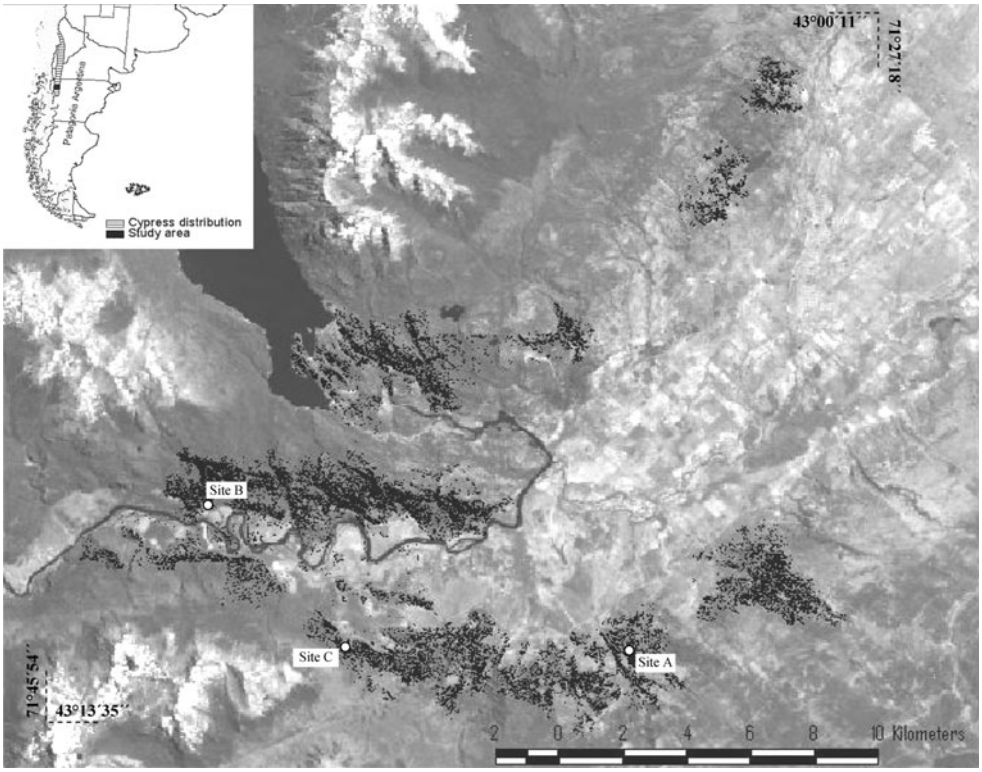

Fig. 1 Location of the study area

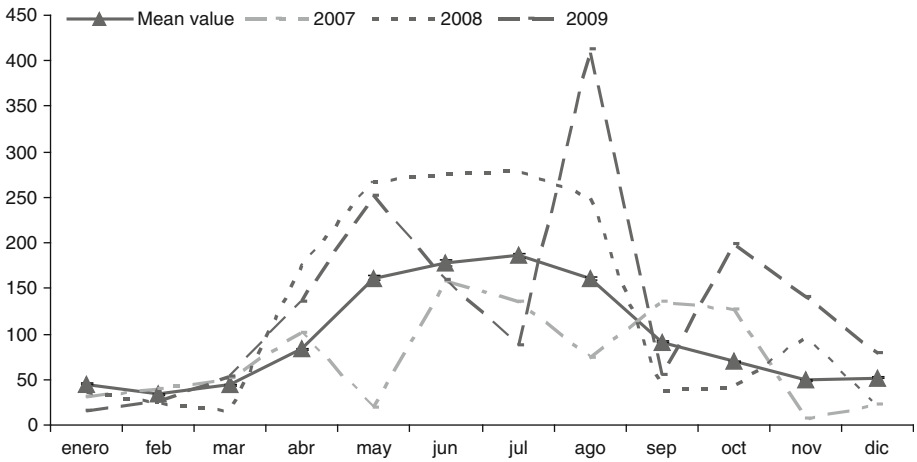

Fig. 2 Precipitation distribution during the study period, and mean historical values registered by the Futaleufú Dam weather station

particle size was determined by passing the sample through 4-, 2-, 1-, 0.5-, 0.25-, 0.09- and 0.045-mm sieves. Texture according to Bouyoucos (1962) and pH NaF 1 N were determined for fractions finer than 2 mm.

In each plot, all cypress individuals with diameter at breast height (DBH) greater than 5 cm were mapped with an electronic distance measure device using a Cartesian coordinate system. Individuals were characterized by DBH and health condition. Basal area was calculated from DBH. Health condition was classified as asymptomatic, live-affected and dead. Living trees with more than 30% of defoliation were considered as live-affected. Although defoliation was the main symptom considered for characterizing the health condition, a quick survey of red-brown necrotic lesions in the inner bark, typical of *Phytophthora* attacks (Greslebin and Hansen 2010), was assessed by performing two incisions at the lower bole. Trees showing stem necroses with less than 30% of defoliation were also considered as live-affected. The proportion of trees showing stem necroses without defoliation was low, varying between 0 and 3% of diseased trees. The health condition was evaluated on January in 2007, 2008 and 2010. During the first sampling, ELISA immunoassays were performed in samples of lesions from three trees in order to confirm the presence of *P. austrocedrae* in the plot (Greslebin and Hansen 2010).

Hegyi's competition index (Hegyi 1974) was calculated for each tree considering as competitors those trees located

within a distance up to 5 m, in accordance with Navarrete Espinoza et al. (2008). We evaluated the association between the health condition and the Hegyi's index with Kruskal–Wallis test.

Spatial statistics analyses of trees in different soil types

The mapped point pattern of asymptomatic and symptomatic (live-affected + dead) trees was characterized by means of spatial statistical techniques. A commonly used characterization of point pattern is the second-order neighborhood analysis based on bivariate *K*-function $K_{12}(r)$, defined as the expected number of points of pattern 2 within a given distance r of an arbitrary point of pattern 1, divided by the intensity λ_2 of points of pattern 2, where intensity is the mean number of points per unit area. The pair correlation function $g_{12}(r)$ is the analog of Ripley's $K_{12}(r)$ when replacing the circles of radius r by rings with radius r and fixed width. The Wiegand–Moloney's *O*-ring statistic $O_{12}(r) = \lambda_2\, g_{12}(r)$ gives the expected number of points of pattern 2 at distance r from an arbitrary point of pattern 1 (Wiegand and Moloney 2004). In this study, we prefer to use the $g_{12}(r)$ since it is noncumulative, and hence, it does not integrate the 'memory' (i.e., trend at lower r) of small-scale second-order effects to larger scales (Wiegand and Moloney 2004; Djossa et al. 2008).

To determine the statistical significance of the observed $g_{12}(r)$, 99 Monte Carlo simulated replicates of the appropriate null model were used for defining 95% confidence envelopes (Stoyan and Stoyan 1994). The appropriate null model to test asymptomatic and symptomatic trees spatial distribution is random labeling. This null model verifies whether or not the labels "type 1" (represented here by asymptomatic trees) and "type 2" (represented by symptomatic trees) have a random structure within the given spatial structure of the joined pattern. With this null model, we avoid misinterpreting spatial patterns that may not be related to the disease distribution, but with the spatial pattern of the forest itself (for example, availability of seeds). Numerical implementation of the random labeling null model involves repeated simulations using the fixed $n_1 + n_2$ locations of patterns 1 and 2, but randomly assigning "case" labels to n_1 of these locations (Bailey and Gatrell 1995). Therefore, the expected bivariate g function under random labeling is the univariate g function of the joined pattern. We evaluated the variant $g_{21}(r) - g_{22}(r)$. The difference $g_{21}(r) - g_{22}(r)$ evaluates whether type 2 points (symptomatic trees) tend to be surrounded by other points of type 2. Thus, a negative difference indicates that rings with radius r around type 2 points contain relatively more type 2 than type 1 points. The term "relatively" refers to the correction that considers the different intensities of patterns 1 and 2. In other words, negative values of the difference $g_{21}(r) - g_{22}(r)$ indicate that type 2 points are positively correlated with other type 2 points (Wiegand 2004).

The spatial analyses were run using Programita software created by Wiegand and Moloney (2004). Analyses were run separately for each plot and for the merged plots of each site. Thus, for each soil type and year of sampling, the data from the replicate plots were combined into one overall mean weighted pair correlation function (Diggle 2003), with the "Combine replicates" option. In all analyses, we used a 0.5-m cell size, which is a fine enough resolution to answer our questions, and a ring width of 3 cells. We calculated the statistics up to a scale of 20 m (40 cells) taking into account plot size (Wiegand 2004; Wiegand and Moloney 2004).

Disease spatial pattern and microsite features

The spatial distribution of the disease was evaluated in relation to microsite features by multivariate analysis. For each study site, a principal component analysis (PCA) was conducted with those topographic and edaphic features varying within the plots and relevant for each soil type, and the Hegyi's competition index (Hegyi 1974). The microsite properties and the average of Hegyi's index in the twenty-four 10 × 10 m subplots of each plot were considered for the analysis. The correlation between the PCA axes and the percentage of diseased trees (live-affected + dead) in each subplot was evaluated by Spearman test.

Disease progression

Changes in the mapped point pattern of asymptomatic and symptomatic trees during the study were characterized by spatial statistical techniques. The spatial pattern of disease progression was evaluated under the null model "Random labeling under antecedent condition", which assumes that the two types of points were created in sequence, the type appearing in the first place is independent of the type created next. Under this model, the bivariate O-ring statistic investigates whether or not new diseased trees (point pattern 2; i.e., asymptomatic trees that became live-affected or died) are more frequent than healthy trees (pattern 0) in the neighborhood of cells occupied by previously diseased trees (point pattern 1) (Xu et al. 2009). The analysis was run using Programita software (Wiegand and Moloney 2004). Data from the replicate plots of each soil type were combined (Diggle 2003).

The variables associated with the disease progression were identified through a discriminant analysis. The analysis was run for trees classified as asymptomatic in the first sampling and considering two groups (i.e., dependent variables): trees becoming diseased during the study period

and trees remaining asymptomatic. The independent variables were the distance to a previously diseased tree, those topographic and edaphic features varying within the plots and relevant for each soil type, and the Hegyi's competition index (Hegyi 1974). A stepwise procedure was used to retain the most significant variables for discrimination (Afifi and Clark 1984).

Influence of precipitation and soil on the progression of symptoms

The percentage of asymptomatic trees becoming live-affected and the mortality rate (i.e., change from asymptomatic or live-affected to dead) during the study period were compared between the soil types by nonparametric Kruskal–Wallis test, and between the dry and wet years by Wilcoxon signed ranks test.

The symptoms progression rate was calculated according to Sheil et al. (1995) as

$$[1 - (1 - N_{\text{lost}}/N_{\text{o}})^{1/t}] \times 100$$

being N_{lost} the number of trees that became dead or affected during time t and N_{o} the number of alive or asymptomatic trees at time 0. The value of t is "1" for 2007 and "2" for 2008–2009 period.

Results

Forest structure

The sampling sites showed different forest structure, as indicated by DBH, basal area and the number of trees per ha (Table 1). All the plots presented a high level of disease incidence. The pair of plots showed a similar disease incidence for Sites B and C. Disease incidence in Site A plots was high but differed in each of them (Table 1). Since soils were similar in both plots, the differences might correspond to factors other than edaphic features, such as the date of entry of the pathogen or different disease progression rates.

Sites description

Site A: Clay soils

Soils of sampling Site A originated from volcanic ash with a glacifluvial lithological discontinuity of clay deposits (Table 2). Soil profiles described in the subplots were similar to those described in Table 2, with variations in slope, presence and depth of redoximorphic features, depth of the clay discontinuity and percentage of rock fragments. Slope varied from 1° to 26° and aspect was Southwest (220°). Redoximorphic features were absent in some profiles, and they appeared from 25 cm depth in others. All profiles showed clay discontinuity, and it varied from 16 to 70 cm depth. The reaction to NaF was always negative and NaF pH was lower than 9.2 units, indicating the absence of amorphous clays (Irisarri 2000). Texture according to Bouyoucos (1962) ranged from loam to clay loam at 0–20 cm depth, clay loam to clay at 60–80 cm and clay below 100 cm depth.

Site B: Alluvial soils

Soils of sampling Site B originated from alluvial parent material with ash gain (Table 2). The aspect was Southeast to Southwest. Textures determined in the field varied from silty clay loam to loamy sand. The influence of volcanic ash and the presence of amorphous clay varied greatly between the profiles. In some profiles, lithological discontinuities were observed, with rocks in the upper slope and fine alluvial deposit at the bottom. Thus, there was a strong influence of slope position (upper/middle/bottom) on soil characteristics. Texture according to Bouyoucos (1962) ranged from clay loam to loamy sand at 0–20 cm depth, clay to loamy sand at 60–80 cm and clay to sand at 100–120 cm depth. The coarse textures in depth coincided with the upper slope. The reaction to NaF varied markedly, suggesting the absence of amorphous clays in some profiles and presence of allophane in others.

Site C: Volcanic and rocky soils

Soils of sampling Site C derive from volcanic ashes (Table 2). The subplots presented North aspect (10° to 355°), and were located in a steep slope ranging up to 50°, and a complex microtopography. Textures determined both in the field and according to Bouyoucos (1962) were sandy loam all along the profiles. All the profiles presented allophane and rock fragments, and the volcanic ash deposit varied in depth. Most of the profiles presented a lithologic discontinuity of andesite at less than one meter depth.

Disease spatial pattern and microsite features

Site A: Clay soils

The assessment of spatial pattern through function $g_{21}-g_{22}$ indicated that at very small spatial scale of less than 1.5 m (i.e., 3 cells), symptomatic trees were grouped. These results were similar for both plots over the study period (Fig. 3a). However, at greater scales, both plots differed greatly in the spatial pattern of the disease, even though they have the same soil type. At spatial scales higher than 1.5 m, the distribution of diseased and asymptomatic trees

Table 1 Forest structure in the sampling sites

Plot 1		Disease incidence[a]			Plot 2		Disease incidence		
		2006	2007	2009			2006	2007	2009
Site A									
Trees/ha	156	25%	31%	39%	Trees/ha	288	67%	69%	78%
BA[b]	28	23%	32%	41%	BA	30	54%	55%	65%
DBH[c]	23				DBH	18			
Site B									
Trees/ha	91	59%	63%	74%	Trees/ha	136	49%	55%	60%
BA	54	44%	50%	63%	BA	40	47%	52%	56%
DBH	43				DBH	30			
Site C									
Trees/ha	143	50%	56%	60%	Trees/ha	205	53%	60%	66%
BA	28	55%	62%	66%	BA	55	51%	63%	67%
DBH	25				DBH	29			

[a] Disease incidence: percentage of diseased trees (including live-affected and dead trees)

[b] *BA* basal area (m^2)

[c] *DBH* diameter at breast height (cm)

in plot 1 followed a random pattern, according to the null model of random labeling (Figs. 3a). On the other hand, diseased trees tended to be clustered in plot 2 (Fig. 3b), in which the number of trees per ha and disease incidence were higher (Table 1).

In the PCA, the subplots of both plots were grouped according to the presence of redoximorphic features, slope, rock fragments, depth of the clay horizon and Hegyi's index. Although edaphic and topographic features varied within the plots, the microsite variation was not associated with the percentage of affected trees in the subplots for the first PCA axis ($p > 0.05$) (Fig. 4a). There was no evidence of a significant association between disease incidence and abiotic factors. On the other hand, the second PCA axis was positively related to the percentage of diseased trees ($p < 0.05$), and this axis was correlated with the Hegyi's competition index. Only in the denser plot (plot 2), diseased trees had a higher Hegyi's competition index than asymptomatic trees ($X^2 = 6{,}852$, $p = 0.033$). However, this relationship disappears if trees with DBH < 10 cm are removed from the analysis ($X^2 = 3{,}765$, $p = 0.152$). For plot 1, health condition and competition were unrelated ($X^2 = 1.983$, $p = 0.371$). Competition could be significantly influencing the health condition of smaller diameter trees only in the plot with the largest number of trees per ha (Table 1).

Site B: Alluvial soils

The assessment of spatial pattern through function $g_{21}-g_{22}$ indicated that at small and medium spatial scales (up to 8 or 10 m; i.e., 16 to 20 cells), affected trees were clustered (Fig. 3c). These results were similar for both plots throughout the study period.

In the PCA, the subplots of both plots were grouped according to the presence of redoximorphic features, depth of allophanic ash, the slope position (bottom/middle/upper) and Hegyi's index. Most of subplots with more than 50% disease incidence were located at negative values of the first PCA axis, while all asymptomatic subplots were located at positive values of this axis. The first PCA axis was significantly associated with the percentage of diseased trees (Fig. 4b). Thus, diseased trees were clustered (Fig. 3c) and associated with bottom slope positions and nonallophanized profiles (Fig. 3b). Hegyi's index was related to the second PCA axis and independent of disease incidence. No significant relationship was found between health status and competition index ($X^2 = 4.917$, $p = 0.086$ for plot 1; $X^2 = 1.203$, $p = 0.548$ for plot 2).

Site C: Volcanic and rocky soils

The assessment of spatial pattern through function $g_{21}-g_{22}$ indicated that at small–medium spatial scales (up to 5.5 m), and also at large scales (about 10–15 m), diseased trees were clustered (Fig. 3d). This pattern was similar, but became blurred over time in both plots.

In the PCA, the subplots were grouped according to the depth of ash (always allophanized), the slope gradient, the slope position (plane land vs. slope) and Hegyi's index. A significant negative association between the first PCA axis and disease incidence was found (Fig. 4c). Plots with more

Table 2 Morphological soil properties of sampling sites

Horizon	Depth (cm)	Color[a]	Texture[b]	Structure[c]	Roots[d]	Rock fragments (%)	Redoximorphic features[e]	Boundary[f]
Site A: Los Rifleros—Parent material: ASH on GFD[g]								
Drainage class: Somewhat poorly drained								
Oi	0–2.5							
A	2.5–13	10YR 3/1	l	3 GR M	3 F	0	–	C W
AC	13–35	10YR 3/2	Sil	2 SBK M	2 M	0	–	G W
C1	35–50	10YR 4/1	cl	2 SBK M	1 CO	0	–	A S
2C2	50–78	10YR 5/3	C	2 SBK CO	–	0	m 4 D	
Site B: Río Grande—Parent material: ALL + ASH[g]								
Drainage class: Moderately well drained								
Oi	0–0.3							
A	0.3–21	10YR 3/1	sil	3 GR M	2 F	0	–	G W
AC	21–42	10YR 3/3	sicl	1 GR CO	3 CO	0	–	C S
C	42–80+	10YR 5/3	sl	0 MA	1 M	0	–	
Site C: Los Cipreses—Parent material: ASH on SAP[g]								
Drainage class: Well drained								
Oi	0–3							
A	3–16	10YR 2/1	sl	2 GR M	2 M	2	–	CW
AC	16–36	10YR 3/2	sl	1 SBK F	3 CO	10		GI
C1	36–48	10YR 3/3	sl CNX	1 SBK F	2 F	80	–	GI
2C2	48+		PBY		–	90	–	

[a] Color: Colors are under moist condition according to Munsell soil color charts (1990)

[b] Texture: *c* clay, *l* loam, *cl* clay loam, *sicl* silty clay loam, *sil* silt loam, *sl* sandy loam; *CNX* extremely flagstony, *PBY* para-large bouldery

[c] Structure: 0 = structureless, 1 = weak, 2 = moderate, 3 = strong; *MA* massive, *GR* granular, *SBK* subangular blocky, *F* fine, *M* medium, *CO* coarse

[d] Roots: in black = none, 1 = few, 2 = common, 3 = many; *F* fine, *M* medium, *CO* coarse

[e] Redoximorphic features: in black = none, m = many; 4 = very coarse; *D* distinct

[f] Horizon boundary: *A* abrupt, *C* clear, *G* gradual, *S* smooth, *W* wavy, *I* irregular

[g] Parent material: *ASH* volcanic ashes, *GFD* glacifluvial deposits, *ALL* alluvial deposits, *SAP* saprolite

than 50% diseased incidence tended to be clustered at negative values of the first PCA axis and are found in positions with lower slope and deeper soils. Hegyi's index was related to the second PCA axis and independent of disease incidence. No significant relationship was found between health condition and competition index ($X^2 = 1.091, p = 0.580$ for plot 1 and $X^2 = 2.507, p = 0.286$ for plot 2).

Disease progression

The spatial pattern of disease progression during the study period varied according to the soil type. In clay (Site A) and alluvial (Site B) soils, the pattern was at random at all scales (Fig. 5a, b). On volcanic rocky soils (Site C), the spatial pattern of disease progression showed that asymptomatic trees becoming diseased were located far from previous symptomatic trees at intermediate scales (i.e., O_{12} is below the confidence interval) (Fig. 5c).

The discriminant analysis showed that the distance to a diseased tree is key for determining the disease progression in all sampling sites. Figure 6 shows the groups centroids according to the canonical axis, and the correlation between variables and the canonical axis. The centroid of tree clusters becoming diseased was negatively related to the canonical function, and it was associated with lower values of distance to a diseased tree. On the contrary, the centroid of tree clusters remaining asymptomatic was positively related to the canonical function, and it was associated with a greater distance to a diseased tree. Although the significance for group differentiation varied between the sites, the same trend was observed for the three sampling sites.

For Site A, trees that became diseased were also associated with microsites with lower percentage of rock fragments. For Site C, trees that became diseased were those with lower values of competition index.

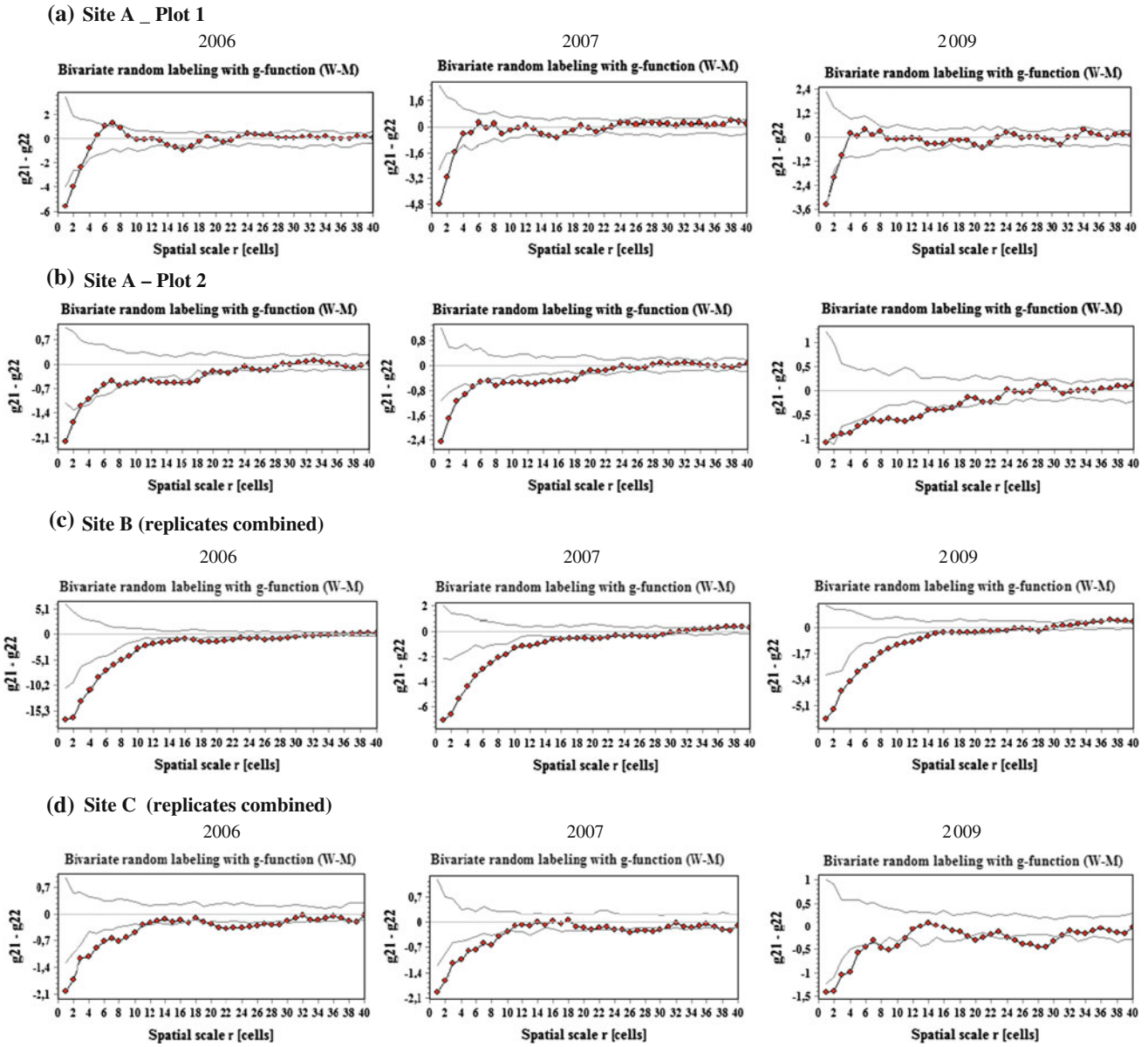

Fig. 3 Results of the bivariate point pattern analysis. Wiegand–Moloney's O-ring statistics (*circle*) and confidence envelopes for Random labeling null model (*solid line*) are shown. Values below the confidence envelope indicate clustering

Influence of precipitation and soil on the progression of symptoms

The annual mortality rate was significantly greater during the wetter years (2008/2009) than during the dry year (2007) ($z = -1.992$; $p = 0.046$). The mortality rate in both plots of a same site was highly variable, with higher values in denser plots (Fig. 7a).

The percentage of asymptomatic trees that became live-affected during the dry year was minimum in clay soils (Site A) and maximum in rocky volcanic soils (Site C), with intermediate values in the alluvial soils (Site B) (Fig. 7b). The same trend was observed in mortality rates (Fig. $4a_2$). During the dry year, no tree died in plot 1 with clay soil (Site A). On the other extreme, 10 trees died (i.e., 42 trees/ha) in plot 2 with volcanic rocky soil (Site C) (Fig. $7a_1$).

In the 2008–2009 period, with precipitation above the historical average, the inverse trend was observed. Despite the erratic response and the lack of significant differences between soil types, the progression of symptoms tended to be greater in clay soils than in volcanic rocky soils (Fig. $7a_2$, b).

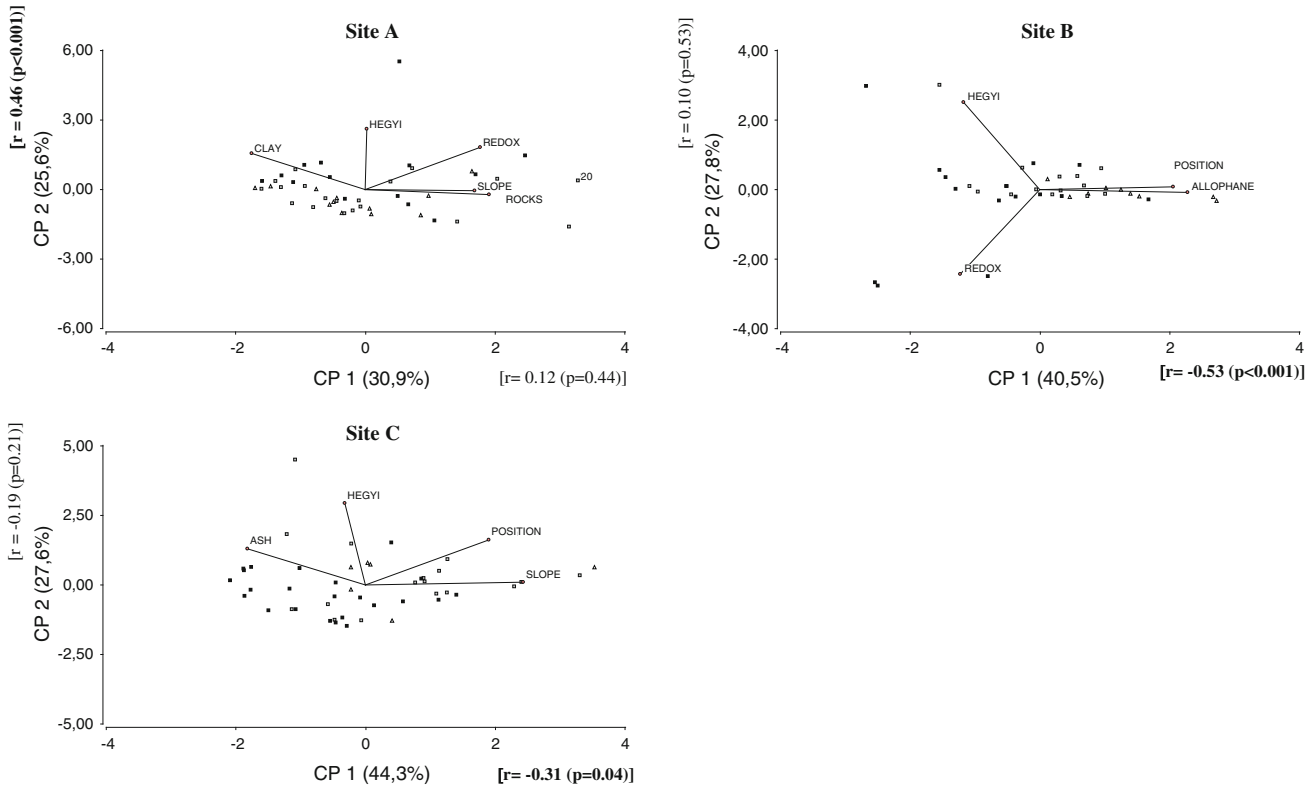

Fig. 4 Subplot principal component analysis (PCA). Each subplot is identified according to the health condition: *triangle* asymptomatic, *gray shaded box* <50% disease incidence, *filled box* >50% disease incidence. Vectors indicate the relationship between the variables and the axes. The correlation between the axes and disease incidence is shown in brackets

Discussion

The spatial pattern of disease was influenced by soil type and tree density. Only in clay soils with low disease incidence, the spatial pattern was random. In clay soils with very high disease incidence (67–78%), the spatial pattern was clustered, possibly as a result of an infection process, rather than being associated with microsite variability. In this case, death by competition could be influencing the health condition of larger trees. In clay soils, disease incidence was not related to microsite variability in abiotic conditions, since all the area could be suitable for disease development. On better drainage conditions, that is, alluvial soils with volcanic ash input and coarse textured volcanic soils, the disease was clustered and associated with flat microtopographies. These results support the proposed hypothesis.

However, over time the disease progressed toward less favorable microsite conditions. The disease progression pattern showed that trees that became diseased during the study period are not significantly closer to diseased trees than asymptomatic trees. This suggests that the disease is progressing on healthy microsites. On the other hand, the discriminant analysis showed that trees that became diseased during the study are those nearest to previously diseased trees. These results suggest that the disease is progressing by a contagion process. In all edaphic situations of our study area, the affected trees were clustered at a small scale (<1.5 m), also suggesting a contagion process. The spatial evidence of contagion from tree to tree is expected since it is in the infected tissues where *Phytophthora* form resistance structures (oospores) that persist in the soil and germinate when conditions are suitable. Thus, the inoculum is concentrated around affected trees (Hansen et al. 2000).

In this study, we see three photographs of the disease spatial pattern, but the pattern may change over time. On clay soils of this study area, the disease appeared in a suitable site for disease development and had a random pattern whenever the incidence of disease was lower, and the spatial pattern became clustered, possibly as a consequence of a contagion process, where the disease incidence was greater. On the other hand, on volcanic rocky soils (Site C), the disease progressed both by a contagion process, according to discriminant analysis, and also far from previously diseased trees as shown by the spatial pattern analysis. The progression in the last case was downslope. This evidence suggests that the spores are swept downslope by runoff, as occurs with other forest diseases caused by *Phytophthora* (Weste 1983; Hansen et al. 2000). This

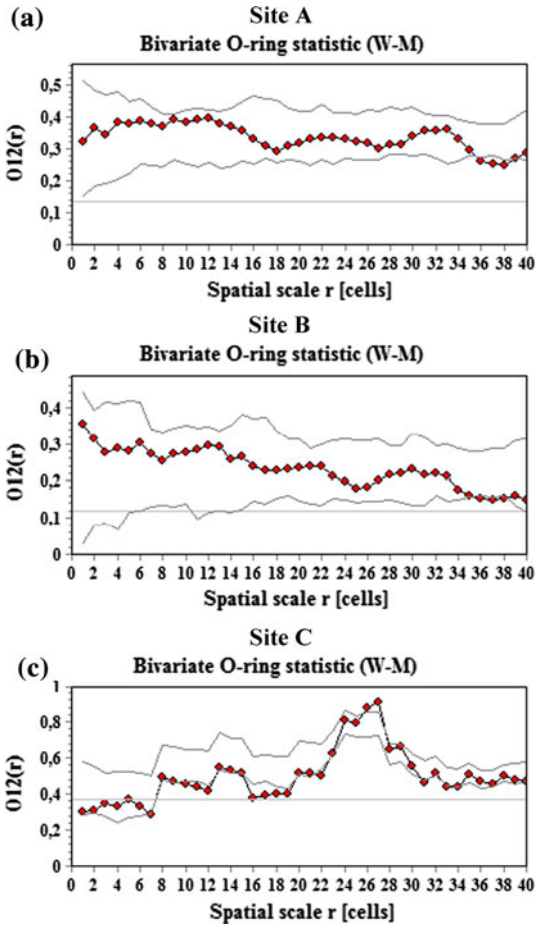

Fig. 5 Results of the bivariate point pattern analyses for disease progression in combined replicates. Wiegand–Moloney's O-ring statistics (*circle*) and confidence envelopes for random labeling under antecedent condition null model (*solid line*). Values between the confidence envelopes indicate that new diseased trees are not more frequently found in the neighborhood of cells occupied by previously diseased trees than healthy ones

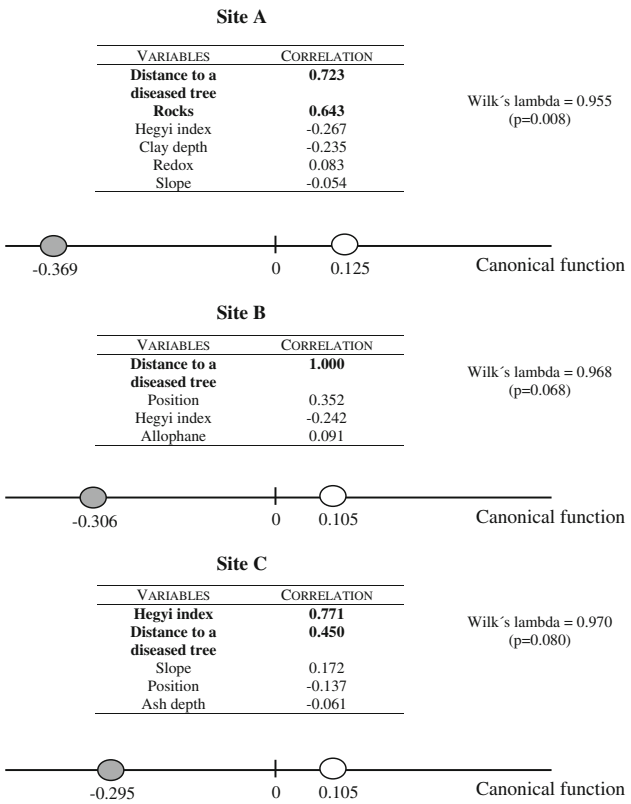

Fig. 6 Results of discriminant analysis, considering two groups: *gray shaded circle* trees becoming diseased during the study period, *open circle* trees remaining asymptomatic. The *tables* show the correlation between the canonical axis and the site variables. Variables in *bold* are those included in the analyses according to the stepwise method

progression should modify the spatial pattern of the disease. On well-drained volcanic soils of Nahuel Huapi National Park, the disease presented an aggregated pattern whenever the incidence of mortality was lower (52–62%) and a random pattern whenever the incidence increased (70–81%) (Rosso et al. 1994).

At landscape scale, the spatial pattern of *A. chilensis* disease was strongly correlated with topographic and soil conditions (La Manna et al. 2008, 2012, La Manna and Matteucci 2010). At stand scale, as that considered in this study, spatial pattern and its relation to site seem to vary over time. Other studies showed that spatial and temporal patterns are more strongly correlated at landscape scale than at the scale of individual trees (Powers et al. 1999).

Although our study reflects short-term responses, results showed that spatial and temporal patterns of disease progression are associated with a contagion process and with environmental variables that affect drainage, corroborating the hypothesis. The progression of symptoms was influenced by soil type and precipitation, and this topic should be evaluated for a longer period. In turn, the weight of annual variability in the disease progression emphasizes the importance of assessing the influence of climate change on mortality.

The annual mortality rates significantly increased during wet years, compared with the dry year. Annual mortality rate varied between 0 and 9.2%, reaching values greater than those found in the last decades to the North of our study area (Amoroso and Larson 2010). Both extreme values correspond to the forests developed on clay soils: 0% for the dry year and 9.2% for the denser plot during the wet years. The maximum value of the rate of asymptomatic trees that became live-affected also corresponded to the denser plot of clay soils during the wet years (16.4%).

The lowest progression of symptoms found in clay soils during the dry year could be associated with less free water because of the highest water retention in clay soils (Narro Farías 1994). This result is expected for a disease caused by *Phytophthora* since soilborne *Phytophthora* species require high soil moisture, which varies with soil type (Weste 1983). The sporangia production in the soil depends on a

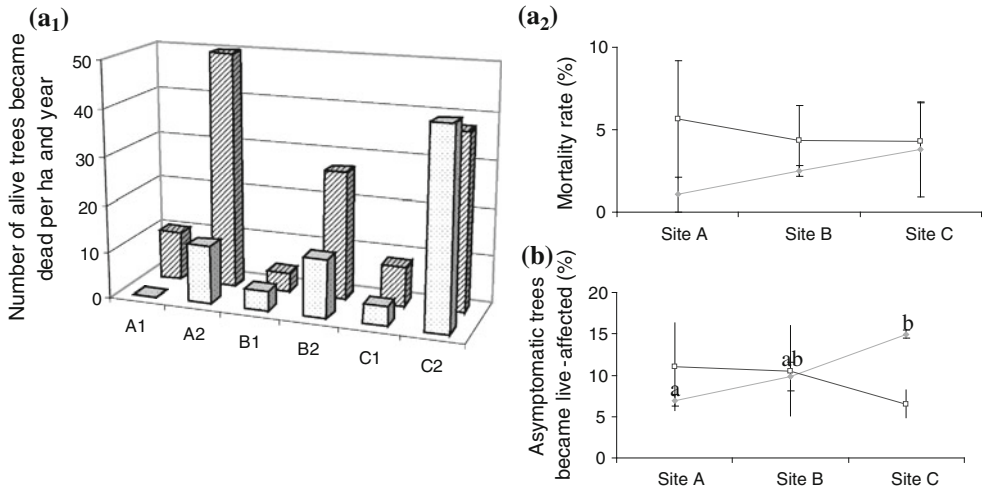

Fig. 7 Progression of symptoms. Figures indicate (**a1**) number, and (**a2**) percentage of live trees that became dead per year. *Figure* (**b**) indicates the percentage of asymptomatic trees that became live-affected per year. *Capital letters* identify the site, and *numbers* identify the plots. *Different letters* in graphic (**b**) indicate significant differences ($p < 0.05$). Study period: 2007 (*dotted bar*), 2008–2009 (*crossed bar*)

sufficiently low water potential. A rainfall that is sufficient for sporangial formation and zoospore release in a sandy soil may not be enough in a clay soil (Reeves 1975; Gisi et al. 1980). In allophanized volcanic soils, characterized by high water availability (Colmet Dâage et al. 1995), moisture content in dry years would be enough for *Phytophthora* development, and the disease may progress even in the driest years. Thus, in the studied dry year, the disease progression reached the greatest values on the volcanic allophanized soils.

Although the disease's cause is still a matter of discussion (El Mujtar and Andenmatten 2007) and other factors such as cavitation have been proposed as direct causes of this disease (El Mujtar 2009), the patterns found in this study support the hypothesis of *P. autrocedrae* as primary causal agent. If cavitation had been the cause, increase in the progression of disease would have been expected in dry years, primarily in clay soils. Furthermore, if cavitation had been the cause, mortality would have increased in the driest areas of *A. chilensis* distribution, precisely where there is no record of the disease. Although differences in vulnerability to cavitation could have been suspected, ecophysiological studies on this forest species found no difference in this issue between different provenances (Gyenge et al. 2005).

Conclusions

The spatial and temporal patterns described in this study concur with *P. austrocedrae* requirements and point at this pathogen as the cause of the disease. The spatial evidence of contagion from tree to tree and the progression downslope on steep slopes are expected for *Phytophthora* disease.

Antecedents about the onset (Calí 1993; Mundo et al. 2010) and the etiology of *A. chilensis* disease (Greslebin and Hansen 2010; Baldini et al. 2008) suggest that the disease is a complex phenomenon that cannot be restricted to a single cause and situation. However, all the reports about the pathology (Greslebin and Hansen 2010), abiotic factors related to the disease (La Manna and Rajchenberg 2004a, b; La Manna et al. 2008, 2012) and the spatial and temporal pattern of the disease and the soil–precipitation interrelation visualized in this study concur in pointing at *P. austrocedrae* as the cause of *A. chilensis* disease in our study area. Management practices should be urgently applied, acknowledging management of other forests affected by *Phytophthora* (Zobel et al. 1985; Hansen et al. 2000).

Acknowledgments We are grateful to A. Greslebin for enriching discussions about *A. chilensis* disease and to T. Kitzberger for his advice about this study. We acknowledge A. Greslebin and M.L. Velez for ELISA immunoassays and J. Monges and students for their help with the fieldwork. Futaleufú Dam facilitated precipitation data. Administración de Parques Nacionales, Mr. Rowland and Mr. F. Jassimovich allowed the access to the study sites. This research was funded by Agencia Nacional de Promoción Científica (PICTO 36776).

References

Acker SA, Harmon ME, Spies TA, McKee WA (1996) Spatial patterns of tree mortality in an old-growth *Abies-Pseudotsuga* stand. Northwest Sci 70(2):132–138

Afifi A, Clark V, (1984) Computer-aided multivariate analysis. Lifetime Learning Publications, Belmont.

Amoroso M, Larson B (2010) Stand development patterns as a consequence of the mortality in *Austrocedrus chilensis* forests. For Ecol Manage 259(10):1981–1992

Baccalá N, Rosso P, Havrylenko M (1998) *Austrocedrus chilensis* mortality in the Nahuel Huapi National Park (Argentina). For Ecol Manage 109:261–269

Bailey TC, Gatrell AC (1995) Interactive spatial data analysis. Longman, Harlow

Baldini A, Oltremari J, Holmgren A (2008) Efecto de *Cinara cupressi* (Hemiptera: Aphididae) sobre el ciprés de la cordillera (*Austrocedrus chilensis*) después de aplicar control químico. Ciencia e Investig Agrar 35(3):341–350

Bouyoucos GJ (1962) Hydrometer method improved for making particle size analysis of soils. Agron J 54:464–465

Brady NC (1974) The nature and properties of soils. McMillan Publishing Company, New York

Calí SG (1996) *Austrocedrus chilensis*: estudio de los anillos de crecimiento y su relación con la dinámica del "mal del ciprés" en el Parque Nacional Nahuel Huapi, Argentina. Dissertation, Universidad Nacional del Comahue, Bariloche, Argentina

Colmet Dâage F, Lanciotti ML, Marcolín A (1995) Importancia forestal de los suelos volcánicos de la Patagonia Norte y Central. Instituto Nacional de Tecnología Agropecuaria, Bariloche

Diggle PJ (2003) Statistical analysis of spatial point patterns, 2nd edn. Edward Arnold, London

Djossa BA, Fahr J, Wiegand T, Ayihouénou BE, Kalko EK, Sinsin A (2008) Land use impact on *Vitellaria paradoxa* C.F. Gaerten. Stand structure and distribution patterns: a comparison of Biosphere Reserve of Pendjari in Atacora district in Benin. Agrofor Syst 72:205–220

El Mujtar V (2009) Análisis integrado de factores genéticos, bióticos y abióticos para la formulación de una nueva hipótesis sobre la etiología del "mal del ciprés". Dissertation, Universidad Nacional de la Plata. La Plata, Argentina

El Mujtar V, Andenmatten E (2007) "Mal del ciprés": búsqueda de la causa más probable de daño mediante un análisis deductivo y comparativo. Bosque 28(1):3–9

Fieldes M, Perrot KW (1966) The nature of allophane in soils Part 3: rapid field and laboratory test for allophane. N Z J Sci 9:623–629

Filip GM, Rosso PH (1999) Cypress mortality (mal del ciprés) in the Patagonian Andes: comparisons with similar forest diseases and declines in North America. Eur J For Pathol 29:89–96

Gisi U, Zentmyer GA, Klure LJ (1980) Production of sporangia by *Phytophthora cinnamomi* and *P. palmivora* in soils at different matric potentials. Phytopathology 70(4):301–306

Greslebin AG, Hansen EM (2009) The decline of *Austrocedrus* forests in Patagonia (Mal del Ciprés): another *Phytophthora*-caused forest disease. In: Goheen EM, Frankel SJ (eds) Proceedings of the fourth meeting of the International Union of Forest Research Organizations (IUFRO) Working Party S07.02.09, *Phytophthoras* in forests and natural ecosystems. U.S. Department of Agriculture, Forest Service, Pacific Southwest Research Station, Albany, CA

Greslebin AG, Hansen EM (2010) Pathogenicity of *Phytophthora austrocedrae* on *Austrocedrus chilensis* and its relation with "Mal del Ciprés" in Patagonia. Plant Pathol 59(4):604–612

Greslebin AG, Hansen EM, Sutton W (2007) *Phytophthora austrocedrae* sp. nov., a new species associated with *Austrocedrus chilensis* mortality in Patagonia (Argentina). Mycol Res 11(3):308–316

Gyenge J, Fernández ME, Dalla Salda G, Schlichter T (2005) Leaf and whole-plant water relations of the Patagonian conifer *Austrocedrus chilensis* (D. Don) Pic. Ser. et Bizzarri: implications on its drought resistance capacity. Ann For Sci 62:297–302

Hansen EM, Goheen DJ, Jules ES, Ullian B (2000) Managing Port-Orford-Cedar and the introduced pathogen *Phytophtora lateralis*. Plant Dis 84:4–14

Hegyi F (1974) A simulation model for managing jack pine stands. In: Fries J (ed) Growth models for tree and stand simulation. Royal Coll For, Res. Note 30

Hennon PE, Hansen EM, Shaw CG III (1990) Dynamics of decline and mortality in *Chamaecyparis nootkatensis* in southeast Alaska. Can J Bot 68:651–662

Irisarri J (2000) La propuesta de reclasificación de los Andepts de Argentina, de acuerdo al Orden Andisoles. In*:* Proceedings of the workshop soil taxonomy, INTA, AICET, AACS, Buenos Aires

La Manna L (2005) Caracterización de los suelos bajo bosque de *Austrocedrus chilensis* a través de un gradiente climático y topográfico en Chubut, Argentina. Bosque 26(2):137–153

La Manna L, Matteucci SD (2010) Estructura del Paisaje de bosques de *Austrocedrus chilensis* con síntomas de defoliación y mortalidad ubicados en distintos tipos de suelo. In: Menghi M, Matteucci SD (eds) Cambios en la cobertura del suelo. Causas, consecuencias y mitigación. Asociación Argentina de Ecología del Paisaje, Buenos Aires, pp 77–82. Available in: http://www.asadep.org.ar/LibroIIjaep/LaManna.pdf

La Manna L, Rajchenberg M (2002) Patrones espaciales del "Mal del ciprés" y su relación con las características del suelo. In: Proceedings XVIII Congreso Argentino de la Ciencia del Suelo, Puerto Madryn, Argentina

La Manna L, Rajchenberg M (2004a) The decline of *Austrocedrus chilensis* forests in Patagonia, Argentina: soil features as predisposing factors. For Ecol Manage 190:345–357

La Manna L, Rajchenberg M (2004b) Soil properties and *Austrocedrus chilensis* decline in Central Patagonia, Argentina. Plant Soil 263:29–41

La Manna L, Matteucci SD, Kitzberger T (2008) Abiotic factors related to the incidence of *Austrocedrus chilensis* disease at a landscape scale. For Ecol Manage 256:1087–1095

La Manna L, Matteucci SD, Kitzberger T (2012) Modelling potential *Phythophtora* disease risk in *Austrocedrus chilensis* forests of Patagonia. Eur J For Res 131:323–337

Manion PD (1991) Tree disease concepts, 2 edn. Prentice-Hall, Englewood Cliffs

Mundo IA, El Mujtar VA, Perdomo MH, Gallo LA, Villalba R, Barrera MD (2010) *Austrocedrus chilensis* growth decline in relation to drought events in northern Patagonia, Argentina. Trees Struct Funct 24(3):561–570

Narro Farías E (1994) Física de Suelos con enfoque agrícola. Editorial Trillas, México DF

Navarrete Espinoza E, Cárcamo Ojeda J, Novoa Barra P (2008) Modelos de crecimiento diametral para *Austrocedrus chilensis* en la Cordillera de Nahuelbuta, Chile: una interpretación biológica. Ciencia e Investig Agrar 33(3):311–320

Pastorino M, Fariña M, Bran D, Gallo L (2006) Extremos geográficos de la distribución natural de *Austrocedrus chilensis* (Cupressaceae). Bol Soc Argent Bot 41:307–311

Powers JS, Sollins P, Harmon ME, Jones JA (1999) Plant-pest interactions in time and space: a Douglas-fir bark beetle outbreak as a case study. Landsc Ecol 14:105–120

Reeves RJ (1975) Behaviour of *Phytophthora cinnamomi* Rands in different soils and water regimes. Soil Biol Biochem 7:19–24

Rosso PH, Baccalá M, Havrylenko M, Fontenla S (1994) Spatial pattern of *Austrocedrus chilensis* wilting and the scope of autocorrelation analysis in natural forests. For Ecol Manage 67:273–279

Schoeneberger PJ, Wysocky DA, Benham E, Broderson W (1998) Field book for describing and sampling soils. Natural Resources Conservation Service, USDA, National Soil Survey Center, Lincoln

Sheil D, Burslem D, Alder D (1995) The interpretation and misinterpretation of mortality rate measures. J Ecol 83:331–333

Shurtleff MC, Averre CW III (1997) The Plant Disease Clinic and Field Diagnosis of Abiotic Diseases. APS Press, St. Paul

Stoyan D, Stoyan H (1994) Fractals, random shapes and point fields. Methods of geometrical statistics. Wiley, Chinchester

Tilman D (1988) Plant Strategies and the Dynamics and Structure of Plant Communities. Princeton Univ. Press, Princeton

Turner M (1989) Landscape ecology: the effect of pattern on process. Annu Rev Ecol Syst 20:171–197

Weste G (1983) Population dynamics and survival of *Phytophthora*. In: Erwin DC, Bartnicki-Gracía S, Tsao PH (eds) *Phytophthora*: its biology, taxonomy, ecology and pathology. APS Press, St. Paul

Wiegand T (2004) Introduction to Point Pattern Analysis with Ripley's *L* and the *O*-ring statistic using the *Programita* software. User manual, second draft version. (Unedited) Available from T. Wiegand, Department of Ecological Modelling, UFZ-Centre for Environmental Research

Wiegand T, Moloney K (2004) Rings, circles, and null-models for point pattern analysis in ecology. Oikos 104:209–229

Wiegand T, Jeltsch F, Hanski I, Grimm V (2003) Using pattern-oriented modeling for revealing hidden information: a key for reconciling ecological theory and application. Oikos 100: 209–222

Xu X, Harwood T, Pautasso M, Jeger M (2009) Spatio-temporal analysis of an invasive plant pathogen (*Phytophthora ramorum*) in England and Wales. Ecography 32:504–516

Zobel DB, Roth LF, Hawk GM (1985) Ecology, pathology, and management of Port-Orford-cedar (Chamaecyparis lawsoniana). General Technical Report PNW-184. U.S. Department of Agriculture, Forest Service. Pacific Northwest Forest and Range Experiment Station, Portland, p 161